

# EXPERIMENTAL AND NUMERICAL INVESTIGATION OF THE EFFECT OF COMPRESSOR OGV PROFILE ON COMBUSTOR EXIT MEASUREMENTS USING AN ISOTHERMAL, NON-REACTING TRACER

*P. Dhopade<sup>1</sup> - P. Denman<sup>2</sup> - P. Ireland<sup>1</sup> - M. Ravikanti<sup>3</sup>*

<sup>1</sup>Department of Engineering Science, University of Oxford, Oxford, United Kingdom,  
priyanka.dhopade@eng.ox.ac.uk

<sup>2</sup>Department of Aeronautical and Automotive Engineering, Loughborough University, Loughborough, United Kingdom

<sup>3</sup>Combustion Systems, Rolls-Royce plc, Derby, United Kingdom

## ABSTRACT

Turbine subsystem cooling design depends on the profile of the non-dimensional temperature distribution function (TDF), measured at a traverse plane upstream of the nozzle guide vane (NGV). To date, the compressor discharge OGV profile was thought to have an insignificant effect on the resulting combustor exit traverse, hence a generic OGV geometry has been used for such tests, which typically remained unchanged between varying combustor designs. The present study however shows that the wake profile of the OGV has a significant influence on the measured combustor exit traverse profile. Experiments were performed at Loughborough University with varying OGV geometries to simulate the aerodynamic field surrounding the combustor. Corresponding numerical analyses were performed using an in-house combustion analysis code with a passive scalar technique to model the CO<sub>2</sub> tracer gas injection and mixing. Analysis of the experimental and numerical simulations confirm that the pressure and velocity profiles presented to the system by an axial flow compressor influence both the mass flow and pressure distributions within the combustor feed annuli. This in turn affects the ratio of the mass flow rates entering the flame tube through the dilutions ports located around the inner and outer annuli. The flow through these ports controls the bulk mixing within the flame tube, resulting in a change in mixture concentration profile measured near the combustor exit. Hence, reproducing engine-representative OGV wake structures for a given engine together with an accurate representation of the combustor configuration is of key importance to reproducing the temperature profiles that inform turbine cooling design.

## NOMENCLATURE

CP Chemically pure  
FSN Fuel spray nozzle  
 $\dot{m}$  mass flow rate (kg/s)  
NGV Nozzle guide vane  
OGV Outlet guide vane  
ppm parts per million  
P Pressure (N/m<sup>2</sup>)  
RIDN Rear inner discharge nozzle  
RODN Rear outer discharge nozzle  
T Temperature (K)  
TDF Temperature distribution function  
U Velocity (m/s)

## subscripts

0 total

n normal/axial direction

$\infty$  mainstream reference temperature

## INTRODUCTION

Knowledge of the temperature profile at the exit of the combustor is vital for turbine cooling system design because of its direct effect on component durability. This is especially critical as progress in modern combustor designs continues to increase turbine inlet temperatures to improve overall engine performance. The velocity of the air approaching the combustor from the HP compressor is typically too high for flame stabilisation, which requires a relatively low velocity (Crook and Horlor, 2005). Hence, a pre-diffuser is used to considerably decrease the velocity of the air entering the combustor flame tube and also to recover as much dynamic pressure as possible in order to provide a smooth and stable flow to the inner and outer annuli. There are two types of widely used pre-diffuser designs: aerodynamic and dump diffusers (Figure 1). The aerodynamic diffuser consists of a long duct to maximise the recovery of dynamic pressure, while reducing the velocity by 35%. The dump diffuser consists of a short diffuser that reduces the velocity by 50%. At the pre-diffuser exit, the air is channelled through the inner annuli, outer annuli and the dome region. Generally, the dump diffuser design is preferred due to a higher tolerance to changes in inlet velocity variations, i.e. variations in OGV exit conditions (Lefebvre and Ballal, 2010). Others have found that this is not strictly accurate, and that annular pre-diffuser designs are sensitive to the inlet conditions delivered to them (Stevens et al., 1984; Klein, 1988). The attraction of the dump pre-diffuser over its fully-faired alternative is stability and length. By allowing the compressor exit flow to separate reliably at the pre-diffuser exit plane, the HP compressor is isolated from the inherent unsteadiness of the flow field surrounding the combustor. Overall pressure losses are minimised by aggressive pressure recovery within the short dump diffuser whilst maintaining its stability.

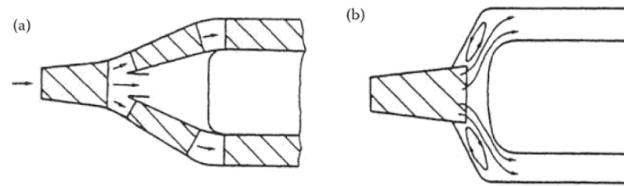


Figure 1: **Annular pre-diffuser designs: (a) aerodynamic and (b) dump. (Lefebvre and Ballal, 2010)**

Once the air enters the flame tube through the swirler dome, modern RQL (Rich-burn/Quick-mix/Lean-burn) design combustors set up a low velocity recirculation zone immediately downstream of the fuel spray nozzle (FSN) for flame stabilisation and utilise large dilution jets to control the  $\text{NO}_x$  and smoke emissions. The region where the flame stabilisation occurs is known as the primary zone and the region where the dilution jets are introduced through intermediate ports is known as the dilution zone of the combustor (Crook and Horlor, 2005).

The effect of the flow field within the flame tube on the downstream combustor-turbine interface and subsequently the HP turbine stages has been studied extensively in the past. For example, Stitzel and Thole (2003) found that the combustor exit total pressure profile significantly affects the development of secondary flow in the turbine, while Simone et al. (2011) found that a non-uniform radial profile of temperature at the combustor-turbine interface significantly increases the blade thermal loading. In the opposite direction, Cha et al. (2012a) investigated the upstream effect of the NGV on the radial profile in the combustor and found that it has a significant impact on the flow velocity and temperature distribution and is highly dependent on the inter-vane spacing. The aerodynamics of the dilution jet mixing in the secondary zone can be complex, depending on the orientation of the jets, and past studies have focused on developing empirical correlations for various configurations of jets (Smith et al., 1991; Holdeman et al., 1988), as well as analysing the effect of the annuli feed on the flame tube internal flow field (Carrotte et al., 2001).

Clearly, the two sub-systems of combustor and turbine are coupled. However, the extent to which the three sub-systems of compressor, combustor and turbine could be coupled still requires further investigation. Recent improvements in the external layout of combustion systems have been achieved with integrated OGV/pre-diffuser designs. For instance, the integrated Outlet Guide Vane (OGV) concept developed by Walker et al. (2007) integrates the OGV with the short dump-style pre-diffuser, resulting in higher feed quality to the annulus regions and overall reductions in pressure loss, but also delivers a significantly different OGV wake profile.

The present study investigates the effect of two different OGV exit velocity profile shapes delivered to a dump-style pre-

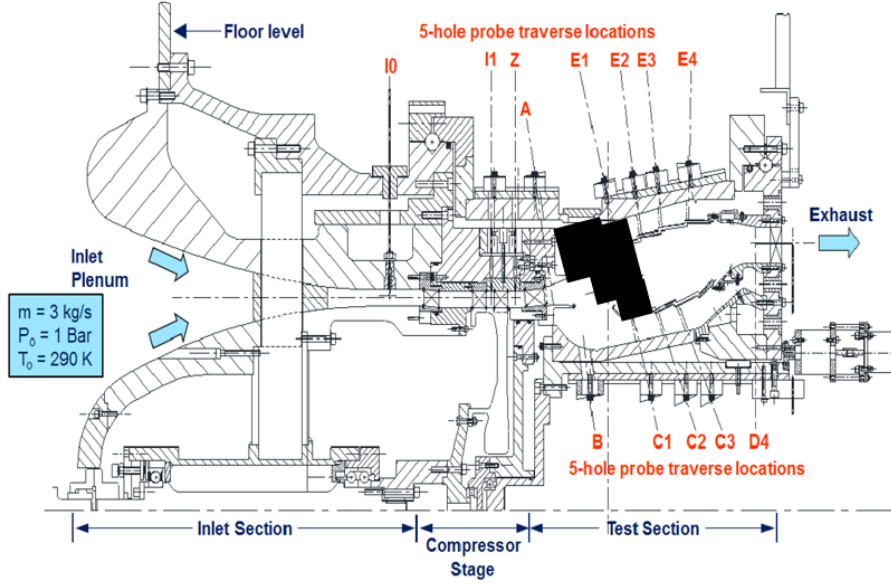


Figure 2: Schematic of annular isothermal test rig at Loughborough University. The region surrounding the FSN has been redacted for proprietary reasons.

diffuser design and examines whether those differences will be convected downstream to the combustor-turbine interface. An engine-representative annular combustor has been utilised for the experimental and numerical investigations. The novel aspect of this study is the direct evaluation of the HP compressor exit conditions on the turbine entry temperature profile, whilst taking into account the complex aerodynamic field within the combustor flame tube and liner. Measurements have been taken in the isothermal annular combustor facility at Loughborough University and numerical predictions have been obtained using the implicit, unstructured, combustion flow solver PRECISE-UNS. The subsequent sections discuss the advantages of isothermal testing, provide more detail on the experimental facility and the numerical treatment.

As per the norm in literature, the temperature distribution functions (TDFs) are used to evaluate the mixing in the temperature field (Cha et al., 2012a):

$$T^* = \frac{T - \bar{T}}{\bar{T} - T_\infty} \quad (1)$$

where  $\bar{T}$  is the area-averaged temperature and  $T_\infty$  is a constant reference temperature.

### Issues with High-Temperature Experimentation

Measurements at the combustor exit are notoriously difficult to make in engine part rigs at an acceptable level of accuracy due to the harsh combustor test rig environment at temperatures up to 2000K with the associated engineering costs. Under full reacting flow conditions, the combustor exit temperature traverse to which the engine HP turbine is to be subjected in service is normally derived by gas analysis in a high-pressure test facility. The inlet section often contains a row of bespoke pre-swirl vanes designed to provide an engine OGV row with an approximation to the approach flow delivered by the last rotor of an HP compressor. The flow entering the pre-diffuser then contains OGV wake structures. With the FSNs passing the correct fuel flow rate and the mixture ignited, gas samples are recovered at the exit plane using a circumferentially swept, water-cooled rake arrangement. The gas temperature at every point is then derived by analysing the constituents of the sample recovered from each passage within the rake. The process is usually repeated at a number of different temperatures and pressures to identify profile changes that may result at different engine operating conditions.

Although these types of tests can often be performed over the correct range of engine operating temperatures, the costs of providing heated air at engine take-off pressures (typically 40 to 50bar) are often prohibitively expensive. Even at lower pressures, the number of tests performed is severely limited by operating costs. In addition, the inlet conditions presented to the engine OGV row in this type of facility are always compromised by a lack of rotating machinery upstream, giving rise to incorrect wake structure and misrepresented radial distributions of pressure/velocity presented to the combustion system under test.

## EXPERIMENTAL FACILITY

Due to the cost, complexity and data collection limitations inherent in all reacting flow test facilities, an alternative method of deriving the exit temperature traverse from rich-burn style combustion systems was sought. For many years at Loughborough, aerodynamic data such as pressure and mass flow distribution surrounding aero-engine combustion systems have been captured using fully annular test rigs such as the one illustrated in Figure 2. Operated under near-ambient, isothermal conditions, these facilities have been employed extensively to investigate the aerodynamic performance of gas turbine combustor diffuser systems in the presence of engine representative outlet guide vane (OGV) wakes. Typically, the wakes are generated using a 1.5 stage axial flow compressor containing an engine OGV row. Generically the requirement is to provide pitch-averaged profiles of pressure, velocity and whirl angle at the OGV entry plane similar to those delivered by a multi-stage HP compressor. In the test rig, this is achieved using a bespoke design of Inlet Guide Vane (IGV) and rotor blade. Moreover, a modular architecture is adopted to enable the compressor and inlet sections to be easily exchanged for those designed specifically to simulate different engine types. Together with this HP compressor simulation, the flow structure delivered by the pre-diffuser to a test section containing the combustor geometry is then very closely replicated.

In the primary zone located upstream of the dilution ports, the highly swirling flow leaving the fuel injectors forms a wide angle cone which in conjunction with the constraining pressure field imposed by the combustor walls causes the flow to impinge on the liner wall upstream of the primary ports. The highly swirling flow also results in a low pressure recirculating flow field located on the centreline of each of the fuel injectors. The resulting pressure field serves to stabilize and locate the flame largely within the primary zone (i.e. swirl stabilized combustion). Flow issuing from a primary located on the centreline of a fuel injector is drawn upstream towards the core of the low pressure region. The extent to which a centreline primary port jet is deflected upstream depends upon the magnitude of the core static pressure relative to the momentum of the jet. In the combusting case, the swirling cone flow in which the heat release takes place causes the stream to accelerate, resulting in a reduction in the fuel injector centreline static pressure relative to the non-combusting case.

As shown in Figure 2, the test section is designed at 1:1 scale to carry a complete engine combustor together with a full set of engine standard fuel spray nozzles (FSN's). The combustor is also pinned to a Perspex outer casing using the same fixing arrangement employed for the engine. Although the annulus flow distribution is imposed largely by the porosity of the combustor, the turbine cooling bleed flows are simulated and set using appropriately sized orifice rings located at the rear of each of the feed annuli. In the engine arrangement, these flows represent the turbine disc, NGV inner and NGV outer cooling flows. In addition, each orifice ring is instrumented and calibrated to determine both the quality of air delivered and the air mass flow rate passing through them. Using this technique, the bleed flows were set to within  $\pm 0.1\%$  of the compressor delivery flow rate. The flows associated with the RIDN and RODN cooling rings are also modelled faithfully using rows of appropriately sized holes positioned in the usual location at the rear of the combustor. For the experiments described in this paper, a complete measurement sector at combustor exit was primarily defined by the liner geometry (i.e. combustor support pins, cooling tile stud patterns etc.).

At the combustor exit plane (i.e. Plane D4 in Figure 2), this area survey was completed by moving a 1.24mm diameter gas sampling tube radially and circumferentially around the test rig centreline. Radial probe positioning was achieved using a stepper motor powered linear guide mounted to the inner casing of the test section. Circumferential probe movement was achieved by rotating the inner casing about the rig centreline using a high-power stepper motor. Where appropriate, flow field pressure/velocity data were gathered at the pre-diffuser exit plane (Plane B in Figure 2) by traversing a pneumatic 5-hole probe in the same manner. Using this traverse arrangement, the positional resolution of the linear traverse was  $\pm 0.025\text{mm}$ , which, together with the data acquisition system, provided a radial positional accuracy of better than  $\pm 0.05\text{mm}$ . Similarly, the drive mechanisms providing circumferential movement enabled the probe to be positioned to within  $\pm 0.05^\circ$  of the desired location.

### CO<sub>2</sub> Gas Scalar Mixing Technique

Experiments conducted earlier to understand and capture the effect of density ratio on wall cooling flows have shown this particular property to be relatively weak in its impact upon effectiveness profiles. As in the present study, these earlier experiments were performed using an annular rig containing a development rich-burn combustor. Although holistically performed at a combustor density ratio of 1.0, the density of the RIDN/RODN flows could be adjusted by delivering a mixture of heated air and CO<sub>2</sub> to a manifold immediately above the entry to the coolant holes. Using this technique, the coolant to mainstream density ratio could be varied from 1.0 up to about 1.3 at a constant momentum flux ratio (i.e. wall pressure drop) and blowing ratios similar to that of the engine. Although still slightly lower than the engine local density ratio of 1.45, the data reveal that in this combustor-like environment, coolant to mainstream density ratio is of second order. In view of these measurements, it has been considered that the turbulent mixing processes within the rich-burn combustor, and which is responsible for delivering the exit traverse, are largely a result of isothermal processes. The main assumption here is that the large scale mixing dominated by the large dilution jets is the primary mechanism behind the combustion process. Just as importantly however, these isothermal mixing processes are strongly influenced by the external flow field surrounding the combustor and therefore, the flow conditions delivered to the system by the HP compressor OGV/pre-diffuser (Carrotte



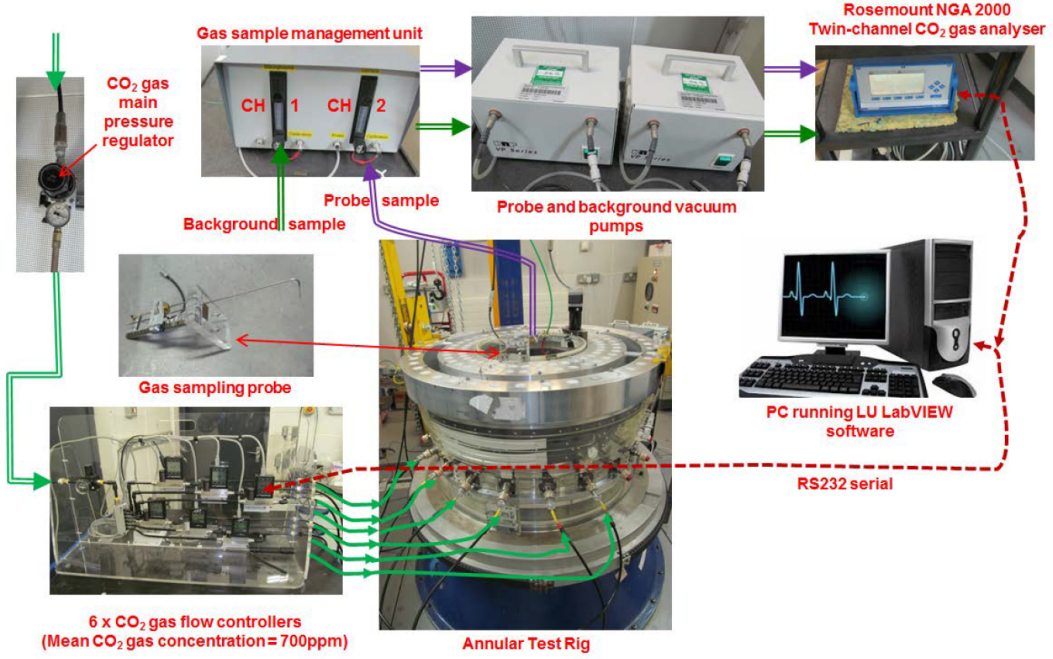


Figure 3: CO<sub>2</sub> gas delivery and sampling system.

et al., 2001). In view of this, the annular test rigs at Loughborough offer the potential to deliver exit traverse data by simple isothermal gas tracing at near-ambient conditions (Denman and Ireland, 2010; Cha et al., 2012a,b). To capitalise on this potential however, a suitable scalar to replace temperature needed to be identified and a method of introducing it determined. For the scalar, CO<sub>2</sub> gas was chosen for its ease of availability, relatively low cost and safety in low concentrations. In addition, the simplest way of delivering the trace gas into the combustor primary zone was thought to be via the liquid fuel gallery within existing FSN engine hardware. With this basic arrangement, a suitable instrumentation system could be specified and designed, the result of which is illustrated in Figure 3.

As indicated in Figure 3, CP grade CO<sub>2</sub> gas is delivered to the liquid fuel passages of six air spray-type FSN's via the individual gas flow controllers. A suitable gas injection rate to the module was chosen based upon the test rig operating condition, the resulting air mass flow rate delivered to the combustor exit plane (Plane D4 in Figure 2) and the dynamic range of the infrared analyser. For the experiments described here, the resulting CO<sub>2</sub> gas flow rate delivered to each FSN was approximately 4.5 litres/min (STP) providing a mean concentration of 700 parts per million (ppm)  $\pm 0.2\%$ . The gas samples are delivered to each channel of the analyser at a constant flow rate of approximately 1.0 litre/min using the two small vacuum pumps shown in Figure 3. The exact flow rate of the sample gas removed from the measurement plane is determined by the requirement to remove the sample isokinetically. The two-channel IR gas analyser enables simultaneous measurements of traverse plane and background CO<sub>2</sub> concentration to be recorded at every measurement point. The temporal performance of the gas analyser, together with this sample delivery system, provides an overall  $t_{90}$  response time of approximately 15 sec. Applying this probe settling time to the measurement process, the response of the analyser beyond the  $t_{90}$  point can be corrected easily using channel calibration data. Channel response and errors due to the influence of ambient temperature and pressure on the calibration of the analyser are corrected by administering span and zero reference gases prior to each experiment. Using this experimental arrangement and procedure, repeatability of the gas distribution contours recorded in these experiments was found to be better than  $\pm 2\%$ .

The CO<sub>2</sub> gas concentrations are normalised similar to the TDF in Equation 1:

$$CO_2^* = \frac{CO_2 - \overline{CO_2}}{\overline{CO_2}} \quad (2)$$

where  $\overline{CO_2}$  is the area-averaged CO<sub>2</sub> concentration.

## Operating Conditions

The software, instrumentation, data acquisition and control systems used to perform the experiments presented here were developed within at Loughborough University and are described in detail by Denman (2002). Using these systems, all three axial flow rig compressors were operated at a constant non-dimensional speed ( $N\pi D/\sqrt{\gamma RT_{01}}$ ) and at a flow coefficient ( $V_a/U_{blade}$ ) of within  $\pm 0.18\%$  of their design values. At this condition, the inlet Mach number to each compressor remained

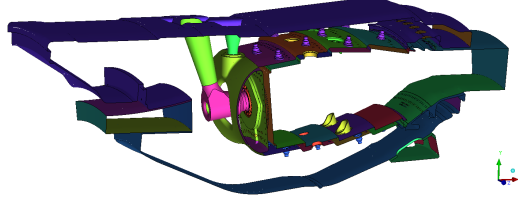


Figure 4: Geometry details of engine representative annular combustor sector used in present study.

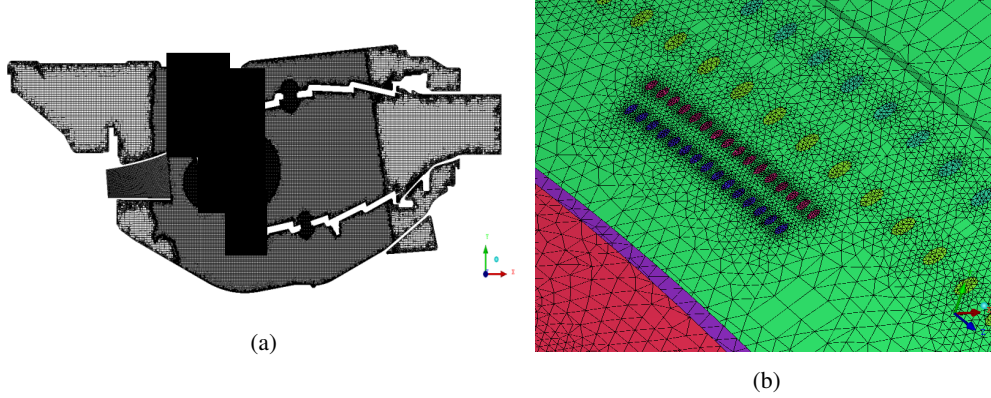


Figure 5: Mesh details of engine representative annular combustor sector used in present study: (a) 2-D section plane through hexa-core periodic mesh (b) RIDN holes along inner annulus surface. The region surrounding the FSN has been redacted for proprietary reasons.

constant at approximately  $0.2 \pm 0.08\%$  and the Reynolds number based upon the OGV chord at mid-annulus height was close to  $1.8 \times 10^5$ .

## NUMERICAL PROCEDURE

The industry in-house code PRECISE-UNS (Predictive-System for Real Engine Combustors - Unstructured) is an implicit, finite-volume, unstructured CFD flow solver for low Mach number flows. It contains the capability to solve the chemical flow reactions involved with combustion, as well as non-reacting flows. For the purpose of this study, only the non-reacting, steady-state isothermal flow has been resolved using the Reynolds-Averaged Navier Stokes (RANS) model, along with a passive scalar tracking technique within PRECISE-UNS, to obtain mixture profiles at the traverse plane. The solver has previously been validated extensively (Anand et al., 2013).

### Computational Domain and Grid

The domain consists of a periodic sector, shown in Figure 4. Each sector contains one FSN. The dump diffuser is shown upstream of the FSN, and the OGV exit profile has been interpolated onto the inlet boundary of the pre-diffuser. The traverse plane axial location is identical to that of the experimental rig (Plane D4).

The computational grid was generated using ANSYS ICEM CFD v16.2. A combination of unstructured multi-block and hexa-core meshes was used for the domain, resulting in a total of 23.7 million elements. The pre-diffuser was meshed using a single block with hexa elements, while the remainder of the domain was meshed using the hexa-core meshing algorithm. The hexa-core meshing algorithm uses the unstructured robust-octree method and then replaces the tetrahedral elements outside of the near-wall region with hexahedral cells. The surface mesh contains a combination of tetrahedral and hexahedral elements. No boundary layers were generated for the current domain, since the very low speed flow near the walls of the flame tube was not considered to be critical to the mixing process occurring in the central region of the flame tube. A 2D section through the mid-circumferential plane is shown in Figure 5(a), where left to right is in the positive axial direction.

High density regions of elements were used near the FSN and swirler vane assembly, as well as through the dilution ports. A slightly less dense region was bounded by the pre-diffuser exit and the traverse plane location in the axial direction. Additionally, each of the RIDN and RODN holes is also represented and are illustrated in Figure 5(b). The relatively high element count of the mesh was required to resolve the RIDN and RODN flows. These features required a relatively small minimum element size of 0.25mm, approximately 12.5% of the global element seed size.

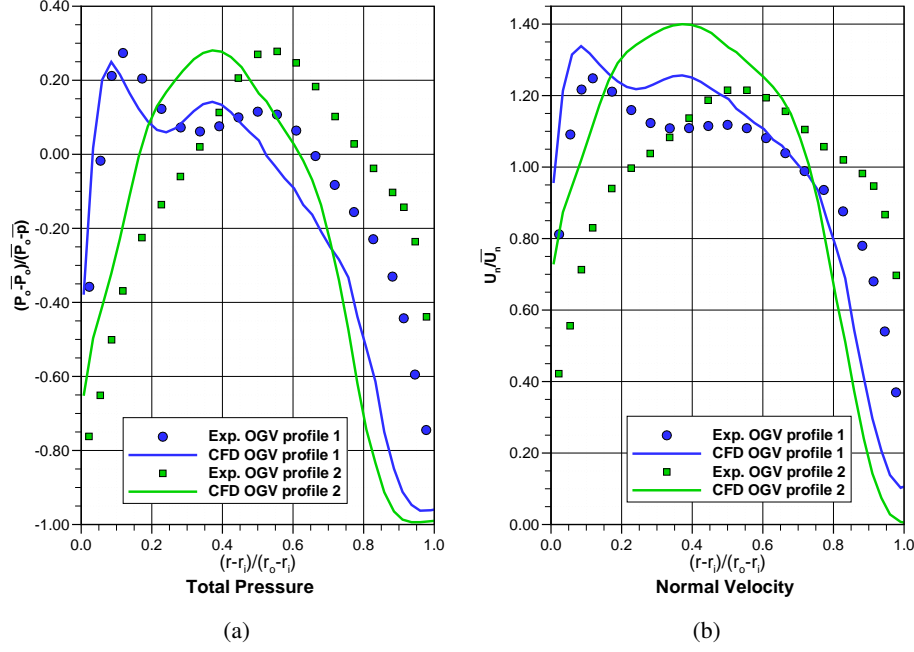


Figure 6: (a) Total pressure and (b) Normal velocity at OGV exit for Profile 1 and Profile 2, circumferentially averaged across one sector.

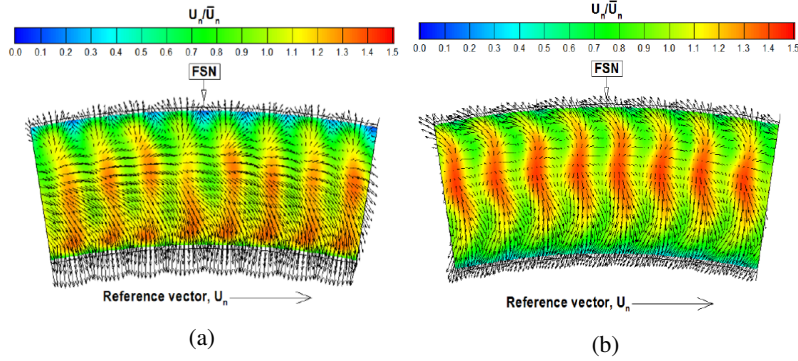


Figure 7: Experimental normal velocity contours for (a) OGV profile 1 (b) OGV profile 2.

### Spatial discretisation, boundary conditions and passive scalar tracking

The second-order linear upwind scheme was chosen for velocity and first-order upwind scheme for turbulent kinetic energy, the details of which are described in Weckering (2011). The realizable  $k-\epsilon$  model was used to simulate the turbulence. At all of the boundaries, except the pre-diffuser inlet, constant mass flux conditions were imposed. The flow-splits were calculated using a semi-empirical network code, which will not be described in detail in this paper. At the pre-diffuser inlet, the OGV exit wake profile was imposed using velocity components and turbulence kinetic energy levels. The profile was obtained from previously completed 3D steady flow calculations of the HP compressor stages using the HYDRA flow solver (Giles et al., 2003), performed by the industry partner.

The mixture concentration profiles in the isothermal simulations were calculated using a passive scalar tracking technique for the mass concentration of the scalar within PRECISE-UNS, where the scalar was assumed to have identical properties to the surrounding airflow, and injected through the FSN swirler along the FSN centreline. The passive scalar transport equation was solved using a method similar to that of Kim and Moin (1989) for turbulent flows. Since the  $\text{CO}_2$  in the experiments was assumed to have minimal effect on the surrounding flow, the experimental  $\text{CO}_2$  concentration and numerical passive scalar concentration can be considered to be equivalent, and therefore compared.

### COMPRESSOR OGV EXIT PROFILES

The circumferentially averaged inlet profiles to the combustor across one sector are shown in Figure 6. These profiles have been measured/computed at the exit plane of the pre-diffuser. The experimental and numerical profiles are compared

for the two different OGV designs, where profile 1 is a standard, non-integrated engine-representative OGV design, and profile 2 is an integrated OGV design, similar to that of Walker et al. (2011). The total pressure has been normalised by the mass-averaged total pressure and dynamic head, whilst the normal velocity (normal to the radial plane) has been normalised by the area-averaged normal velocity on the pre-diffuser exit plane. The key point to note is that the characteristic shape of the profiles for both quantities has changed from a hub-biased one to that of a centre-biased shape. The experimental and numerical profiles are in good agreement for profile 1, where the peak occurs at approximately 10% of duct height. There are differences in profile 2, for both the total pressure and normal velocity curves, likely due to the fact that both experimental and numerical profiles supplied by the industry partner were for slightly different sub-iterations of engine models, with subtle differences in performance. The difference in experimental and numerical peak value of normal velocity for profile 2 is 13%. The experimental profile 2 is center-biased around 55% of duct height, whilst the numerical profile 2 is center-biased around 37% duct height. This will be of importance later during the discussion of the scalar distribution profiles.

Examples of the flow structure measured at pre-diffuser exit and delivered to the combustor test sections by both rig compressors are shown in Figure 7, where the sector is centered around the burner centerline. Here, in-plane velocity vectors are plotted together with normalised axial velocity to illustrate the difference between the conventional, non-integrated compressor simulation and the integrated alternative. The hub-biased nature of conventional design is immediately apparent from the contours, as is the enhanced flow deflection towards the engine centreline. A flow field like this gives rise to an imbalance of pressures between the inner and outer feed annuli surrounding the combustor and as a result, dilution ports and wall cooling flows are fed by better quality air on one side of the combustor than the other. In the case of profile 1, the inner feed annulus is preferentially fed in terms of pressure. In the case of the integrated design in profile 2, the flow at pre-diffuser exit is much more evenly distributed radially giving rise to near equal pressures within the inner and out feed annuli of the combustor. With similar combustor geometries located downstream, changes will be expected in the pressure field surrounding each of them to have an influence on the exit temperature traverse delivered to the HP turbine.

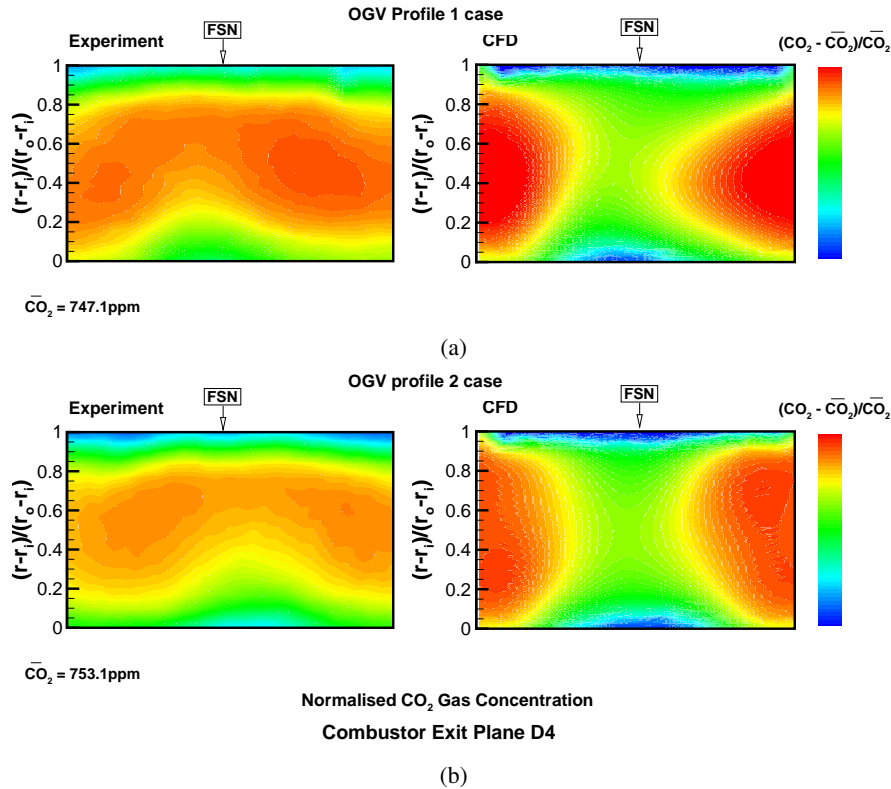


Figure 8: Contours of  $\text{CO}_2$  concentration on traverse plane D4 for both cases with (a) OGV profile 1 and (b) OGV profile 2. The circumferential coordinates and concentration values have been omitted for proprietary reasons.

## RESULTS AND DISCUSSION

### Passive scalar fields

The results at the traverse plane D4 are discussed first. Figure 8 shows the experimental and numerical traverse plane concentrations of  $\text{CO}_2$  for a single sector. In Figure 8(a), which corresponds to the OGV profile 1 case, two “hotspots” are clearly visible in both experimental and numerical predictions. This is not surprising, as these hotspots are governed by the



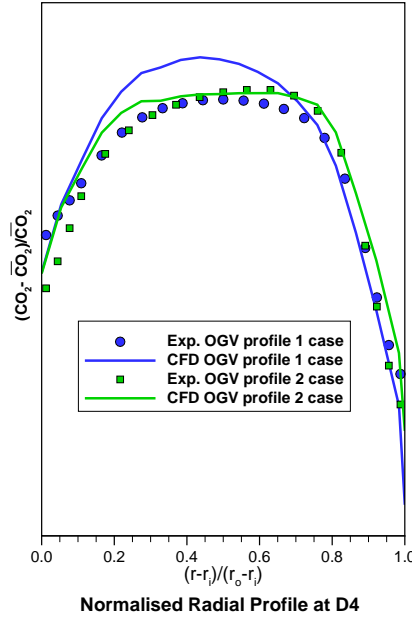


Figure 9: Circumferentially averaged CO<sub>2</sub> concentration at traverse plane D4. The concentration values have been omitted for proprietary reasons.

circumferential arrangement of the dilution ports (Cha et al., 2012a). The intensity of the hotspots is predicted to be higher in the CFD, and in between the two hotspots, the CO<sub>2</sub> concentration is predicted to be lower than the experiments, resulting in a less “mixed-out” region around the burner centreline. This is likely due to the turbulence quantities being solved using a first-order linear upwind scheme, however this was necessary to achieve a stable solution. A qualitative assessment shows that both the experiment and CFD show a mixture concentration that is biased towards the inner wall.

In Figure 8(b), corresponding to the OGV profile 2 case, the two hotspots still exist, however have shifted towards the 50% duct height centreline, indicating a more radially uniform mixture profile away from the endwalls. This is further re-iterated in Figure 9, which shows the circumferentially averaged, normalised profile of the CO<sub>2</sub> concentration for both experimental and numerical cases. The shape of the radial profiles for each case is consistent across both experimental and numerical simulations. For the OGV profile 1 case, the peak concentration level is lower in the experiment compared to the CFD prediction. For the OGV profile 2 case, the match is much better in terms of peak and outer wall concentration levels. Comparing the two numerical cases, the profile shapes are significantly different, with the OGV profile 2 case resulting in a flatter concentration near 50% duct height, with a lower peak concentration level than that of OGV profile 1. The change between the two profiles is less obvious through the experimental data, however the largest change occurs at the inner annulus endwall and near 70% duct height. At the inner endwall, OGV profile 1 case (with the hub-biased pre-diffuser inlet profile) measures a CO<sub>2</sub> concentration level that is higher than OGV profile 2.

Another key result is that although the experimental and numerical OGV profiles for case 2 (Figure 6) have peaks at 55% and 37% duct height, respectively, they still result in similarly flat exit traverse profiles, compared to the hub-biased profile 1. This suggests that there exists a threshold in the radial plane around which the OGV exit can be centred, which would result in a different balance of pressures around the inner and outer annuli of the combustor feeding the dilution ports. An OGV exit profile biased towards a point below this threshold would result in the inner annulus ports being fed preferentially (as evidenced by the profile 1 case), and vice versa. This is likely to be a factor of the cant angle of the pre-diffuser with respect to the burner centerline, i.e. dependent on the combustor geometry. For instance, in an integrated design, the vanes are leant circumferentially to direct the flow to the match the combustor cant angle before it leaves the vane row. This leads to a centre biased profile. In a non-integrated system, the pre-diffuser must accommodate the cant angle whilst diffusing which generally gives rise to a hub-biased profile. The error in IR analyser measurement is about 0.5% of reading and this translates to about  $\pm 0.011$  in terms of an error bar for all profile plots derived from  $(CO_2 - CO_{2bar})/CO_{2bar}$ .

## Numerical analysis

Figure 10 shows the CFD predictions of normalised mass flow rates entering the inner and outer annuli for both cases. The annular planes were taken just upstream of the primary dilution ports. The values were normalised by the inlet mass flow rate into the combustor. For the case with OGV profile 1, a higher feed into the inner annulus is predicted. This trend is reversed for OGV profile 2, with a smaller difference, indicating a more equal feed delivered to the dilution ports.

Figure 11 illustrates the normalised velocity magnitude in and around the combustor at two fixed circumferential posi-

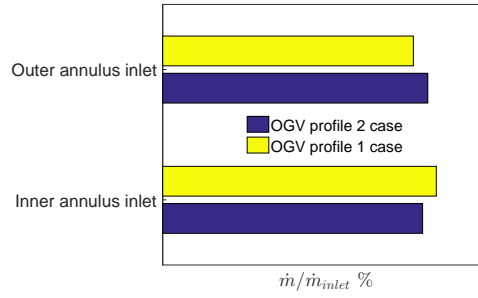


Figure 10: Normalised mass flow rates entering the inner and outer annuli for both cases with OGV profile 1 and OGV profile 2 from the numerical simulation.

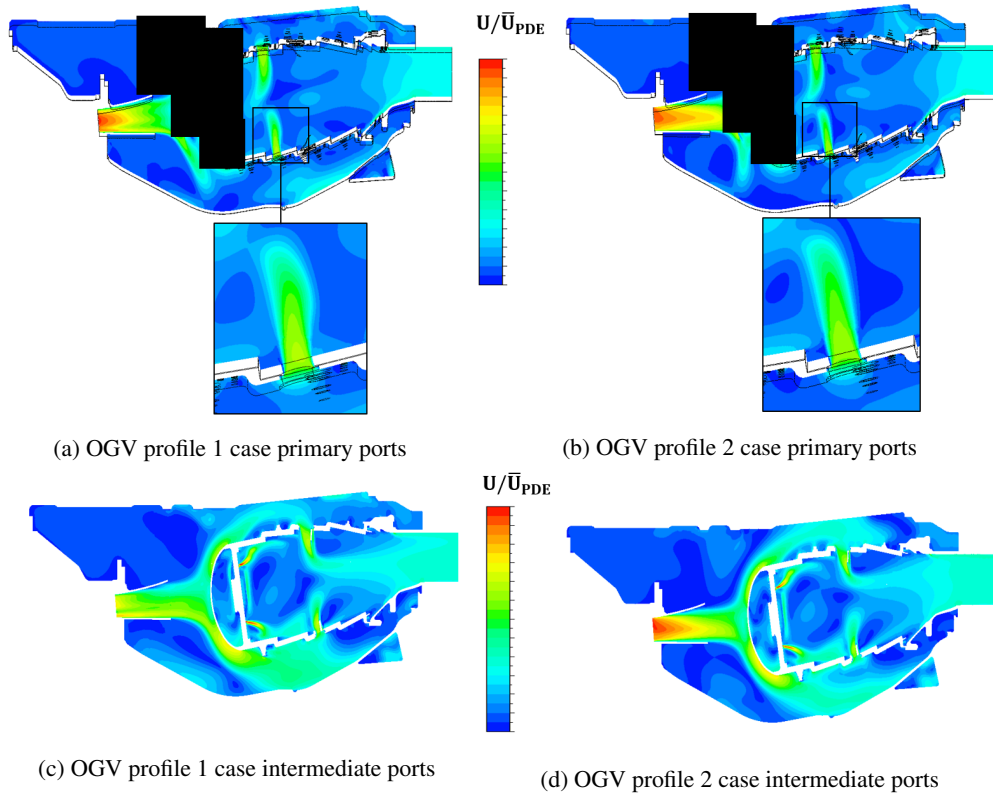


Figure 11: CFD predictions of normalised velocity magnitude along centreline plane that bisects the FSN and primary dilution port for (a) OG profile 1 case (b) OG profile 2 case and centreline plane that bisects the intermediate dilution port (c) OG profile 1 case and (d) OG profile 2 case. The region surrounding the FSN has been redacted for proprietary reasons.

tions. The velocity magnitude has been normalised by the area-averaged value at the pre-diffuser exit plane for both cases. Figures 11(a) and 11(b) show the flow distribution at a plane along the FSN and primary dilution port centreline. The turning of the flow into the inner annulus is clearly visible for the profile 1 case, compared to the profile 2 case, where the flow appears to turn radially inwards at a steeper angle. The magnified inset with the primary inner dilution port reflects the change in shape due to this change in annulus feed, where the profile 2 case experiences a more slender jet.

In Figures 11(c) and 11(d), the normalised velocity magnitude is shown in the plane that bisects an intermediate port (the dilution port arrangement was illustrated in Figure 4). Here, the preferential flow into the inner annulus is clearly visible for profile 1, while the more equal distribution around the annuli is seen for profile 2. This also changes the dilution jet dynamics, resulting in varying mixture profiles, as evidenced by Figure 12.

Figure 12 shows contours of the  $\text{CO}_2$  concentration at the same two planes from Figure 11. To illustrate the decreasing concentration from the injection point, the concentration was non-dimensionalised using the area-averaged value at the injection point, so that the concentration level at the injection point is equal to one. The colour scale has been saturated at the high concentration values in the primary zone to better visualise the changes in the intermediate and dilution zones. The

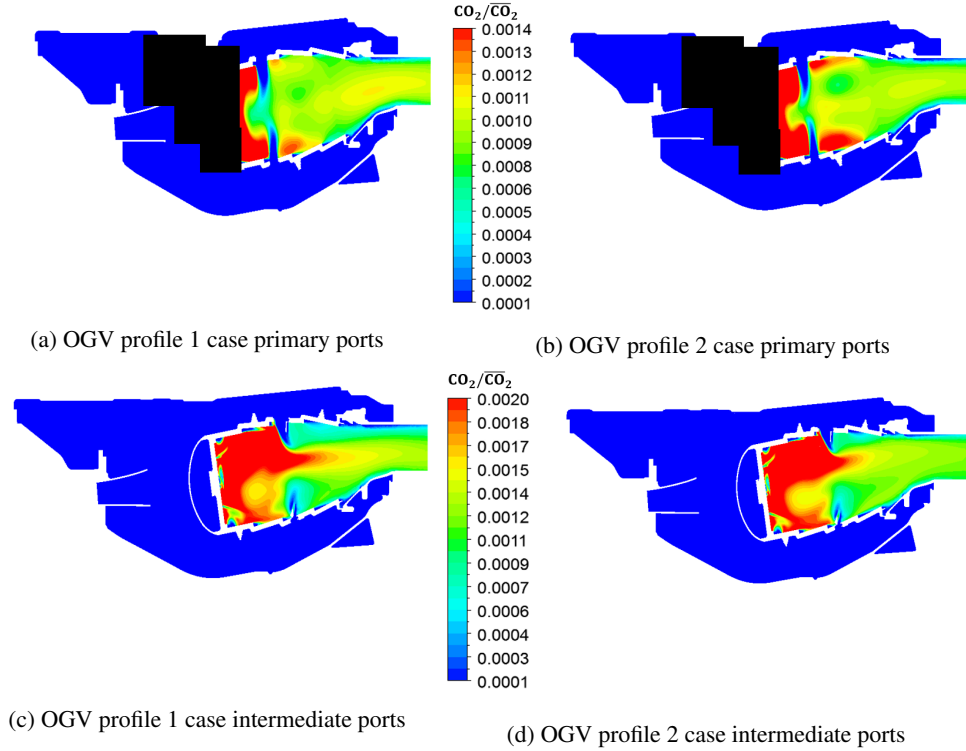


Figure 12: **CFD predictions of  $\text{CO}_2$  mixture fraction along centreline plane that bisects the FSN and primary dilution port for (a) OGV profile 1 case (b) OGV profile 2 case and centreline plane that bisects the intermediate dilution port (c) OGV profile 1 case and (d) OGV profile 2 case. The region surrounding the FSN has been redacted for proprietary reasons.**

flow through the primary ports shows similar concentration levels approaching the ports, but a slightly larger region of lower concentration for profile 1. This suggests that the better fed inner annulus primary ports aid in the combustion process in the primary zone. However, Figures 12(c) and 12(d) show that the intermediate ports have a significant effect on the mixing and any differences in the port feeds dictate the changes in the downstream concentration. A possible mechanism for the differences is that the inner intermediate ports for profile 1 have a higher core velocity, therefore a lower static pressure and higher dynamic head than profile 2, given that both cases are subjected to identical magnitudes of total pressure (but a different radial distribution). The decrease in static pressure around the inner annulus intermediate ports could have a potential entrainment effect which causes the unmixed core to turn downwards, as visible in Figure 12(c). Whereas the ports in profile 2 case are more equally fed around the annulus, resulting in a better balance of pressure and increased mixing in the intermediate and dilution zones.

## CONCLUSIONS

An isothermal near-ambient mixing technique has been developed to simulate the exit traverse delivered by a rich-burn combustor to the entry of the HP turbine. The test vehicle employed for this purpose is a fully annular facility originally developed to provide combustion engineers with pressure and mass flow distribution data around engine combustor hardware. Facilities of this type include an LP axial flow rig compressor specifically designed to provide flow structures and profiles to the test section containing the combustor that are similar to those of the engine. Designed at 1:1 scale, the test section is able to accommodate engine liners, together with a complete set of engine fuel spray nozzles.

Adopting an aerodynamic facility of this type, gas tracing at very low concentration has been employed to reproduce the exit traverse of a rich-burn combustor with two different upstream compressor geometries. In both cases, the approach conditions were provided by a test rig compressor specifically designed to simulate the flow delivered by the engine HP machine. Two such compressor designs were used to deliver different OGV exit profiles to the pre-diffuser, one based on a legacy, non-integrated OGV/pre-diffuser design (OGV profile 1) and another representative of a more modern, integrated design (OGV profile 2).

A numerical analysis was performed on the same model of combustor, with OGV exit profiles imposed on the pre-diffuser inlet plane of the domain. The in-house flow solver, PRECISE-UNS, was used to compute the isothermal flow field with a passive scalar tracking method to predict the tracer gas concentration. In situations where the upstream pre-diffuser conditions are different, the pressure field surrounding the combustor is altered and as a result, the energy available to drive port flow

mixing and wall cooling is redistributed. This effect becomes even more significant in situations where the combustor wall pressure drop is reduced, as is the case for modern combustion systems.

The numerical analysis shows that the inlet mass flow rates to both the inner and outer annuli are altered with the radial distribution of the OGV exit profiles. A more hub-biased OGV exit profile results in a more preferentially fed inner annulus, while a more centre-biased profile results in a more equal distribution around the annulus. In addition, the theory of a threshold is proposed for the radial location of the OGV exit profile peak, below which the flow is biased towards the inner annulus, leading to a less mixed-out exit traverse profile and beyond which results in a flatter exit traverse profile. This is evidenced by the fact that for the profile 2 case, the numerical OGV exit profile is less centre-biased than the experimental profile, yet both combustor exit traverse profiles agree well.

The apparent importance of upstream boundary conditions on exit traverse simulation would suggest greater attention must be placed upon replicating the flow structures and profiles of velocity and pressure delivered to the system. This is extremely difficult to achieve in stator cascades such as those employed on reacting flow rigs. Tip leakages above the rotor and below cantilevered stator vanes cannot be replicated and the interaction between pre-swirl vane wakes and the OGV row is almost unavoidable. Modern OGV/pre-diffuser systems are also aerodynamically integrated and fail to function properly without the influence of rotating machinery upstream.

These conclusions therefore suggest that the fidelity with which the flow conditions leaving the pre-diffuser must be replicated is important if temperature traverse delivered by the combustor to the HP turbine is to be accurately simulated. In the cases where the rotor is not present, the stator vane should not be the original one but rather, one that replicates the outlet flow angle distribution and wake profile.

## ACKNOWLEDGEMENTS

The authors would like to acknowledge the support of Rolls-Royce plc under the SILOET II framework. The author would also like to thank Christopher Goddard and Marco Zedda from Rolls-Royce plc for their help with PRECISE-UNS.

## References

- Anand, M. S., Eggels, R., Staufer, M., Zedda, M., and Zhu, J. (2013). An advanced unstructured-grid finite-volume design system for gas turbine combustion analysis, GTINDIA2013-3537. In *ASME 2013 Gas Turbine India Conference*, page V001T03A003.
- Carrotte, J. F., Griffiths, J. P., and Spencer, A. (2001). Primary jet characteristics within an isothermal gas turbine combustor, 2001-GT-0057. In *ASME Turbo Expo 2001: Power for Land, Sea, and Air*, volume 2: Coal, Biomass and Alternative Fuels; Combustion and Fuels; Oil and Gas, pages V002T02A024–35.
- Cha, C. M., Hong, S., Ireland, P. T., Denman, P., and Savarianandam, V. (2012a). Experimental and numerical investigation of combustor-turbine interaction using an isothermal, nonreacting tracer. *Journal of Engineering for Gas Turbines and Power*, 134(8):081501.
- Cha, C. M., Ireland, P. T., Denman, P., and Savarianandam, V. (2012b). Turbulence levels are high at the combustor-turbine interface. GT2012-69130. In *ASME Turbo Expo 2012: Turbine Technical Conference and Exposition*, volume 8, Parts A, B and C. American Society of Mechanical Engineers.
- Crook, G. and Horlor, M. (2005). *The Jet Engine*. Wiley-Blackwell, Rolls-Royce plc, 5th revised edition.
- Denman, P. A. (2002). Aerodynamic evaluation of double annular combustion systems, GT-2002-30465. In *Proceedings of ASME Turbo Expo, Amsterdam, The Netherlands*.
- Denman, P. A. and Ireland, P. (2010). SAMULET Task 1.3.3: Interdependency of the combustor-turbine interface, Interim Report D1.3.3.3. Technical report, Loughborough University Report TT10R016.
- Giles, M. B., Duta, M. C., Muller, J.-D., and Pierce, N. A. (2003). Algorithm developments for discrete adjoint methods. *AIAA Journal*, 41(2):198–205.
- Holdeman, J. D., Srinivasan, R., and White, C. D. (1988). An empirical model of the effects of curvature and convergence on dilution jet mixing. techreport, NASA Lewis Research Center.
- Kim, J. and Moin, P. (1989). *Transport of Passive Scalars in a Turbulent Channel Flow*, pages 85–96. Springer Berlin Heidelberg, Berlin, Heidelberg.
- Klein, A. (1988). The relation between losses and entry flow conditions in short dump diffusers for combustors. *The Aeronautical Journal*, 92(920):390–396.
- Lefebvre, A. and Ballal, D. (2010). *Gas Turbine Combustion*. CRC Press, 3rd edition.
- Simone, S., Montomoli, F., Martelli, F., Chana, K., Qureshi, I., and Povey, T. (2011). Analysis on the effect of a nonuniform inlet profile on heat transfer and fluid flow in turbine stages. *Journal of Turbomachinery*, 134(1):011012–1 – 011012–14.
- Smith, C., Talpallikar, M., and Holdeman, J. (1991). A CFD study of jet mixing in reduced flow areas for lower combustor emissions. In *Proceedings of 27th Joint Propulsion Conference, Sacramento, California, June 24-27*.
- Stevens, S., Harasgama, S., and Wray, A. (1984). The influence of blade wakes on combustor shortened pre-diffusers. *Journal of Aircraft*, 21:641–648.



- Stitzel, S. and Thole, K. A. (2003). Flow field computations of combustor-turbine interactions relevant to a gas turbine engine. In *ASME Turbo Expo 2003, collocated with the 2003 International Joint Power Generation Conference*, volume 5, pages 175–183.
- Walker, A. D., Barker, A. G., Carrotte, J. F., Bolger, J. J., and Green, M. J. (2011). Integrated OGV design for an aggressive S-shaped compressor transition duct. In *ASME 2011 Turbo Expo: Turbine Technical Conference and Exposition*, volume 7.
- Walker, A. D., Carrotte, J. F., and McGuirk, J. J. (2007). Enhanced external aerodynamic performance of a generic combustor using an integrated OGV/prediffuser design technique. *Journal of Engineering for Gas Turbines and Power*, 129:80–87.
- Weckering, J. (2011). *Development of Numerical Modeling Methods for Prediction of Ignition Processes in Aero-Engines*. PhD Thesis, Technischen Universitat Darmstadt.